AMERICAN SOCIETY FOR MICROBIOLOGY | Infection and Immunity®

MICROBIAL IMMUNITY AND VACCINES

A *Plasmodium* Parasite with Complete Late Liver Stage Arrest Protects against Preerythrocytic and Erythrocytic Stage Infection in Mice

Ashley M. Vaughan,[a] Brandon K. Sack,[a] Dorender Dankwa,[a] Nana Minkah,[a] Thao Nguyen,[a] Hayley Cardamone,[a] Stefan H. I. Kappe[a,b]

[a]Center for Infectious Disease Research, Seattle, Washington, USA

[b]Department of Global Health, University of Washington, Seattle, Washington, USA

ABSTRACT Genetically attenuated malaria parasites (GAP) that arrest during liver stage development are powerful immunogens and afford complete and durable protection against sporozoite infection. Late liver stage-arresting GAP provide superior protection against sporozoite challenge in mice compared to early live stage-arresting attenuated parasites. However, very few late liver stage-arresting GAP have been generated to date. Therefore, identification of additional loci that are critical for late liver stage development and can be used to generate novel late liver stage-arresting GAPs is of importance. We further explored genetic attenuation in *Plasmodium yoelii* by combining two gene deletions, *PlasMei2* and *liver-specific protein 2* (*LISP2*), that each cause late liver stage arrest with various degrees of infrequent breakthrough to blood stage infection. The dual gene deletion resulted in a synthetic lethal phenotype that caused complete attenuation in a highly susceptible mouse strain. *P. yoelii plasmei2*$^{-}$ *lisp2*$^{-}$ arrested late in liver stage development and did not persist in livers beyond 3 days after infection. Immunization with this GAP elicited robust protective antibody responses in outbred and inbred mice against sporozoites, liver stages, and blood stages as well as eliciting protective liver-resident T cells. The immunization afforded protection against both sporozoite challenge and blood stage challenge. These findings provide evidence that completely attenuated late liver stage-arresting GAP are achievable via the synthetic lethal approach and might enable a path forward for the creation of a completely attenuated late liver stage-arresting *P. falciparum* GAP.

KEYWORDS GAP, *Plasmodium*, attenuated, liver stage, malaria, preerythrocytic, protection, sporozoite, vaccine

An effective vaccine against *Plasmodium falciparum* malaria will likely be essential for eradication efforts, but subunit vaccine development utilizing selected parasite antigens has so far shown only modest success (1–7). In contrast, formative experimental trials with humans, using immunization with radiation-attenuated sporozoites (RAS), delivered by the bites of mosquitoes, provided near complete protection against challenge with fully infectious sporozoites (referred to as controlled human malaria infection [CHMI]) (8). More recently, vialed, cryopreserved RAS have been administered intravenously (i.v.) and have conferred robust protection against CHMI, demonstrating the safety and efficacy of this form of vaccination as well as the potential for manufacturing scale-up and a practical means of administration (9). Irradiation causes DNA damage in sporozoites, allowing them to retain infectivity, but upon infection of hepatocytes, the DNA damage causes a block in DNA replication and, in consequence, developmental arrest of the parasite at the trophozoite/early schizont stage. This causes parasite death within the infected hepatocyte or death of both the parasite and the infected cell. Attenuated sporozoites are complex immunogens, containing thou-

Received 28 January 2018 **Accepted** 5 February 2018

Accepted manuscript posted online 12 February 2018

Citation Vaughan AM, Sack BK, Dankwa D, Minkah N, Nguyen T, Cardamone H, Kappe SHI. 2018. A *Plasmodium* parasite with complete late liver stage arrest protects against preerythrocytic and erythrocytic stage infection in mice. Infect Immun 86:e00088-18. https://doi.org/10.1128/IAI.00088-18.

Editor John H. Adams, University of South Florida

Address correspondence to Ashley M. Vaughan, ashley.vaughan@cidresearch.org, or Stefan H. I. Kappe, stefan.kappe@cidresearch.org.

sands of unique parasite proteins, many of which are potential antibody targets against the sporozoite as well as T cell targets against the early-infected hepatocyte. As such, RAS stimulate multipronged adaptive immune responses conferring preerythrocytic immunity against infection, thereby preventing the onset of blood stage infection (10). However, if the live parasite immunogens were able to progress further through liver stage schizogony and thus dramatically increase their biomass, as well as further diversifying their antigen repertoire, they should elicit broader and more robust immune responses than RAS. Indeed, this has been shown for humans by an alternate method of whole parasite vaccination, in which subjects undergoing prophylactic treatment with the blood stage antimalarial chloroquine were immunized with fully infectious sporozoites (12, 13). In this immunization, liver stage development progresses normally but exoerythrocytic merozoites that are released from the liver and infect erythrocytes are killed by chloroquine. This method of whole-parasite immunization engenders sterile protection against CHMI but strikingly requires an approximately 60-fold-lower cumulative parasite dose than RAS (14). However, the continuous administration of an antimalarial drug during immunization can likely not be considered a practical method of vaccination.

Fortuitously, targeted gene deletion technology for *Plasmodium* parasites has allowed for a more precise and controlled means for the creation of attenuated parasites (15). Initial studies of rodent malaria genetically attenuated parasites (GAP) focused on the deletion of genes that were upregulated in infective sporozoites (UIS) (16). The deletion of numerous UIS genes from the parasite genome did not affect sporozoite viability but instead caused early developmental arrest of the parasite in the liver, and these GAPs were robust immunogens, protecting immunized mice from sporozoite challenge (11, 17). A *P. falciparum* early liver stage-arresting triple knockout GAP was created (*p36*$^{-}$ *p52*$^{-}$ *sap1*$^{-}$) and showed no evidence of breakthrough to blood stage infection in preclinical studies (18) and in a recent clinical study showed no breakthrough when administered to volunteers by the bites of approximately 200 infected mosquitoes (19). Further *P. falciparum* GAP that arrest early during liver stage development include *P. falciparum b9*$^{-}$ *sap1*$^{-}$ (20) and *P. falciparum abccc2*$^{-}$ (21), but these GAP have yet to be tested in humans.

Identification of early liver stage-arresting GAP gene knockout candidates relied on the transcriptional profiling of salivary gland sporozoites, which uncovered genes essential for the establishment of a liver stage infection but not necessarily genes that control development and maturation of liver stages. To identify the latter, studies of the rodent malaria liver stage proteome and transcriptome and their comparison with other life cycle stages was conducted and uncovered novel potential GAP gene candidates essential for liver stage development (22). These included a subset of genes encoding enzymes involved in the type II fatty acid synthesis pathway (FAS II), an apicoplast-localized pathway of prokaryotic origin (23). Indeed, deletion of FAS II genes in both *Plasmodium yoelii* and *Plasmodium berghei* demonstrated nearly full liver stage developmental progression through schizogony before late liver stage arrest (24–28). *P. yoelii* FAS II knockouts were completely attenuated, whereas *P. berghei* knockouts showed limited breakthrough to blood stage infection. Immunization of mice with *P. yoelii* sporozoites lacking FAS II (27) resulted in a more potent immune response and superior protection than with an early liver stage-arresting *P. yoelii* GAP (29) and *P. yoelii* RAS (30). Importantly, immunized mice were protected from sporozoite challenge after intradermal immunization, indicating increased potency compared to that of early arresting RAS or GAP. Immunized mice were also protected from a lethal blood stage challenge, thus exhibiting life cycle stage-transcending protection (31). Together, these data suggest that a late liver stage-arresting GAP will be a superior immunogen in humans and a safe, late liver stage-arresting *P. falciparum* GAP would appear to be an ideal live-attenuated vaccine strain. However, efforts to create late liver stage-arresting *P. falciparum* GAP have encountered obstacles since the deletion of genes involved in FAS II unexpectedly led to a complete defect in *P. falciparum* sporogony within the mosquito, precluding its production (32, 33).

TABLE 1 Attenuation of gene knockout *P. yoelii* preerythrocytic stages in BALB/c mice

Parasite name or genotype	No. of sporozoites used for inoculation[a]	Mouse	No. of mice patent[b]	No. of days to patency[c]
1971cl1[d]	1,000	BALB/cJ	3/3	3 (3)
1971cl1[d]	10,000	BALB/cJ	3/3	3 (3)
lisp2$^-$	1,000	BALB/cJ	6/8	5 (4) 7 (2)
lisp2$^-$	10,000	BALB/cJ	7/7	4 (2) 5 (4) 6 (1)
plasmei2$^-$	50,000	BALB/cByJ	0/10	
	200,000	BALB/cByJ	3/30	5 (2) 6 (1)
	500,000	BALB/cByJ	4/30	5 (2) 6 (1) 7 (1)
plasmei2$^-$ *lisp2*$^-$	50,000	BALB/cJ	0/30	
	50,000	BALB/cByJ	0/10	
	200,000	BALB/cByJ	0/29	
	500,000	BALB/cByJ	0/26	
fabb/f$^-$	500,000	BALB/cJ	0/10	
	500,000	BALB/cByJ	0/20	

[a]Salivary gland sporozoites were isolated from infected *Anopheles stephensi* mosquitoes, and mice were i.v. challenged with the listed number of sporozoites.
[b]The number of patent mice per number of mice challenged is indicated. Detection of blood stage patent parasitemia was carried out by Giemsa-stained thin blood smear. Attenuation was considered complete if mice remained blood stage negative for 21 days.
[c]If mice became blood stage patent, the day to patency is listed, with the number of mice that became patent in parentheses.
[d]The marker-free GFP-luciferase-expressing 1971cl1 parasite has a wild-type phenotype in all aspects of the life cycle, including sporozoite infectivity, and was used for the creation of all of the gene knockouts.

In a further effort to create novel late liver stage-arresting GAP, we and others continue to screen gene deletions of liver stage-expressed genes for a phenotype of late liver stage developmental arrest in rodent malaria parasites. Two identified independent gene deletions that lead to late liver stage arrest include *PlasMei2* in *P. yoelii* (34) and *liver-specific protein 2* (*LISP2*) in *P. berghei* (35–37). We tested whether dual deletion of *PlasMei2* and *LISP2* could synergize to create a safe, fully attenuated GAP. Our studies show that *P. yoelii plasmei2*$^-$ *lisp2*$^-$ constitutes a synthetic lethal gene deletion combination that completely attenuates the parasite while maintaining a late liver stage-arresting phenotype. Immunization of mice with *P. yoelii plasmei2*$^-$ *lisp2*$^-$ elicited protective T cell and antibody responses and afforded complete protection against sporozoite challenge as well as stage-transcending protection against a blood stage challenge.

RESULTS

***P. yoelii plasmei2*$^-$ and *P. yoelii lisp2*$^-$ show incomplete attenuation of liver stage development.** *P. yoelii PlasMei2* contains an RNA binding domain (RBD) that shares homology to one of the RBDs in Mei2 (Meiosis inhibited 2), originally described for the fission yeast *Schizosaccharomyces pombe* (38). *PlasMei2* is expressed in cytoplasmic granules of liver stage parasites, suggestive of a role in RNA homeostasis. We have previously shown that deletion of *PlasMei2* in *P. yoelii* 17XNL leads to late liver stage arrest and no evidence of breakthrough to blood stage infection when i.v. dosed with 50,000 *plasmei2*$^-$ sporozoites (34) in highly susceptible BALB/cByJ mice (39). To determine if higher doses could lead to breakthrough, we performed challenges i.v. with 200,000 or 500,000 *plasmei2*$^-$ sporozoites in cohorts of 30 BALB/cByJ mice for each dose and did observe occasional breakthrough to blood stage infection (3/30 at 200,000 and 4/30 at 500,000 [Table 1]). This finding shows that *P. yoelii plasmei2*$^-$ is severely but not completely attenuated in highly susceptible mice given high dose

challenges. We next thought that the simultaneous deletion of two liver stage-expressed genes, each of which causes incomplete attenuation at late liver stage, could achieve complete attenuation by creating a synthetic lethal phenotype, assuming that the lack of each unique gene function could synergize in their detrimental effect on liver stage development. We thus considered further gene candidates and chose to study *LISP2* because it is expressed on the middle-to-late liver stage parasitophorous vacuole membrane and deletion of *P. berghei LISP2* leads to incomplete late liver stage growth arrest (37). We first tested whether *P. yoelii lisp2*$^-$ arrests during late liver stage development by deleting the gene using the recently described clustered regularly interspaced short palindromic repeat (CRISPR)/Cas9 technology (40), which allows efficient editing of the parasite genome. The advantage to this system is that transgenic parasites do not carry a drug susceptibility marker and thus can easily undergo further genetic manipulation. The pYC plasmid (40) was thus used to target *LISP2* for deletion in a marker-free *P. yoelii* 17XNL parasite that constitutively expresses a green fluorescent protein (GFP)-luciferase fusion (41) termed 1971cl1. This allows for the noninvasive analysis of liver stage development in mice using an *in vivo* imaging system (IVIS) and analysis of subsequent transition to blood stage infection in the same animals. Two *P. yoelii lisp2*$^-$ clones from two separate transfections were used for studies, and neither showed defects in any stages of the parasite life cycle (data not shown) except during liver stage development. To determine if *P. yoelii lisp2*$^-$ arrests during liver stage development, groups of BALB/cJ mice were i.v. challenged with either 1,000 marker-free GFP-luciferase-expressing 1971cl1 parent parasites (here referred to as wild type) or 1,000 *lisp2*$^-$ sporozoites, and time to blood stage patency was determined. All wild-type-infected mice became blood stage patent on day 3 after challenge, whereas two of seven *P. yoelii lisp2*$^-$-infected mice did not become patent and the remaining mice showed severe delays to patency, becoming patent between 5 and 7 days after infection (Table 1). When mice were challenged with 10,000 *lisp2*$^-$sporozoites, all mice became blood stage patent from days 4 through 6 (Table 1), demonstrating the incomplete attenuation of *P. yoelii lisp2*$^-$.

The *P. yoelii lisp2*$^-$ *plasmei2*$^-$ GAP exhibits complete late liver stage developmental arrest. Next, we created a *P. yoelii lisp2*$^-$ *plasmei2*$^-$ dual gene deletion parasite by deleting *PlasMei2* in the drug-susceptible *P. yoelii lisp2*$^-$ parasite. Two *P. yoelii lisp2*$^-$ *plasmei2*$^-$ parasite clones from separate transfections were phenotypically analyzed, and as for the single gene deletion parasites, there was no apparent impairment of the parasite life cycle up to the point of liver stage development (see Fig. S1 in the supplemental material). We then compared late liver stage development of the *lisp2*$^-$ *plasmei2*$^-$ dual gene deletion parasite with *lisp2*$^-$ and *plasmei2*$^-$ single gene deletion parasites as well as wild-type parasites. Groups of Swiss Webster (SW) mice were challenged i.v. with 50,000 sporozoites of each strain and liver stage developmental progression was measured based on luciferase activity at 43 h, a time point late in liver stage development but before the complete maturation and liver stage-to-blood stage transition of wild-type parasites. Parasite development, based on luciferase expression was indistinguishable between single and dual gene knockout parasite strains and wild-type parasites (Fig. 1A), suggesting that all three GAP progress to late liver stage development. To further assess the phenotype of liver stage development, parasites were visualized by indirect immunofluorescence assay (IFA) at 43 h of liver stage development, using antibodies recognizing the PVM protein Hep17 and the endoplasmic reticulum protein BiP (Fig. 1B). Liver stages of GAP developed to late schizogony and appeared similar to the wild type based on expression patterns of Hep17 (Fig. 1B). However, the *plasmei2*$^-$ liver stages showed a DNA segregation phenotype and aberrant BiP expression (34), and this phenotype was also observed in the *lisp2*$^-$ *plasmei2*$^-$ liver stages (Fig. 1B). To quantify liver stage growth of the gene knockout parasite lines, liver stage size was determined at 43 h in comparison to that of the wild type (Fig. 1C), and no significant differences were seen among all analyzed strains. Thus, *P. yoelii lisp2*$^-$ *plasmei2*$^-$ GAP retains the late-liver stage arresting phenotype of the single gene deletion parasites and phenotypically resembles the *plasmei2*$^-$ single gene

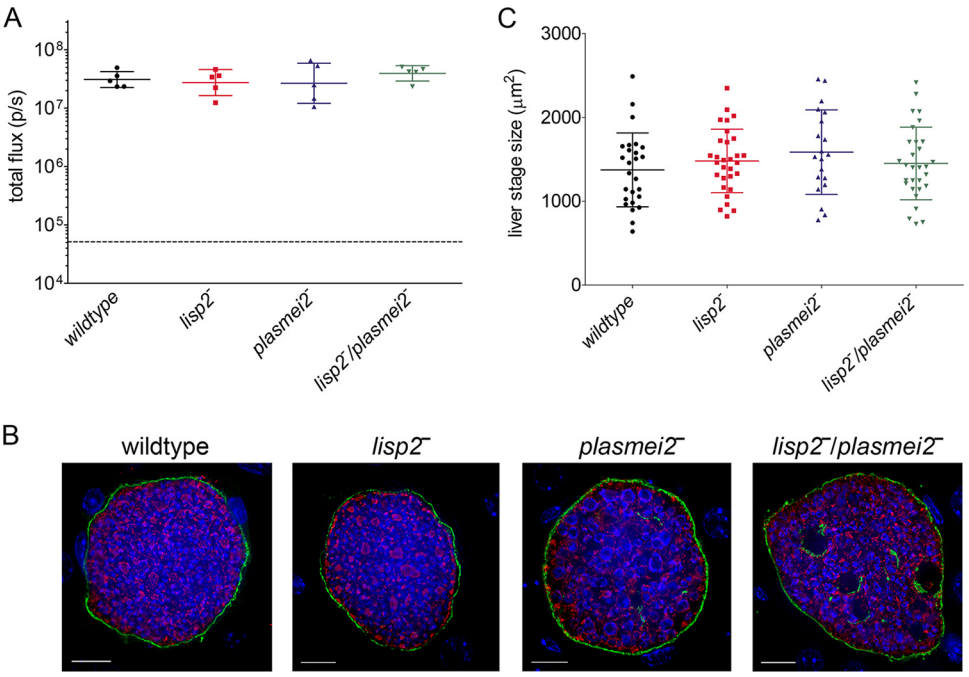

FIG 1 *P. yoelii lisp2*$^-$, *plasmei2*$^-$, and *lisp2*$^-$ *plasmei2*$^-$ GAP arrest late during liver stage development. (A) Groups of five outbred SW mice were i.v. challenged with 50,000 luciferase-expressing GAP sporozoites. As a control, mice were challenged with the luciferase-expressing 1971cl1 parasite, which behaves as the wild type. Liver stage burden was measured *in vivo* at 43 h by assessing luciferase activity (total flux, *y* axis). There was no statistical difference in flux between the four lines, as determined by an unpaired two-tailed *t* test. The dashed line indicates background flux. (B) Livers from parasite-infected mice were harvested, perfused with PBS, and fixed in 4% paraformaldehyde at 43 h after sporozoite infection. Sections (50 μm) were cut from fixed livers, and IFAs were performed using primary antibody to the parasite parasitophorous vacuole membrane (PVM) marker Hep17 (green) and the endoplasmic reticulum (ER) marker BiP (red), and DNA was localized with DAPI (blue). Scale bar: 10 μm. (C) After IFAs were performed, determination of approximate liver stage size (based on area at the parasite's largest circumference using the PVM marker Hep17 as a reference) was calculated in order to make comparisons. At least 20 parasites were assessed at each time point. There was no statistical difference in area between the four parasite lines as determined by an unpaired two-tailed *t* test. The results suggest that all parasites develop at similar rates and thus all GAPs are late liver stage arresting.

knockout (34). To determine whether the *lisp2*$^-$ *plasmei2*$^-$ GAP persisted in the liver, we measured liver stage luciferase activity of the *lisp2*$^-$ *plasmei2*$^-$ GAP over time after sporozoite inoculation in C57BL/6 mice (Fig. 2A). As controls, we compared the *lisp2*$^-$ *plasmei2*$^-$ GAP with both the late liver stage-arresting *fabb/f*$^-$ GAP, created in the GFP-luciferase expressing 1971cl1 parent parasite, and the wild type. All three parasites showed similar luciferase activities at 24 and 44 h after sporozoite inoculation (Fig. 2A); thereafter, wild-type liver stage activity was not measured, as the liver stage-to-blood stage transition occurs at approximately 48 h. At 72 h, both *lisp2*$^-$ *plasmei2*$^-$ GAP and *fabb/f*$^-$ GAP luciferase activities had significantly decreased, with *lisp2*$^-$ *plasmei2*$^-$ GAP activity at background levels, whereas *fabb/f*$^-$ GAP luciferase activity was still significantly higher than background. This suggests that the *fabb/f*$^-$ GAP persists for longer than the *lisp2*$^-$ *plasmei2*$^-$ GAP. At 96 h, both GAP had luciferase activities comparable to background.

To gain further insight into the persistence, yet complete attenuation, of the *lisp2*$^-$ *plasmei2*$^-$ GAP, we estimated the viability of *lisp2*$^-$ *plasmei2*$^-$ liver stages at 36, 42, 48, 54, and 60 h of development by IFA (Fig. 2B) based on the presence of an intact parasitophorous vacuole membrane (PVM). This was delineated by expression of the PVM marker Hep17, and viability was compared to that of the wild-type liver stages at 36, 42, and 48 h, time points when the latter are still present in the liver (Fig. 2B). This assessment of viability was previously used to show the phenotype of the attenuated *plasmei2*$^-$ GAP (34). At 36, 42, and 48 h, the percentage of nonviable *lisp2*$^-$ *plasmei2*$^-$ liver stages was significantly higher than that of the wild type and increased over time

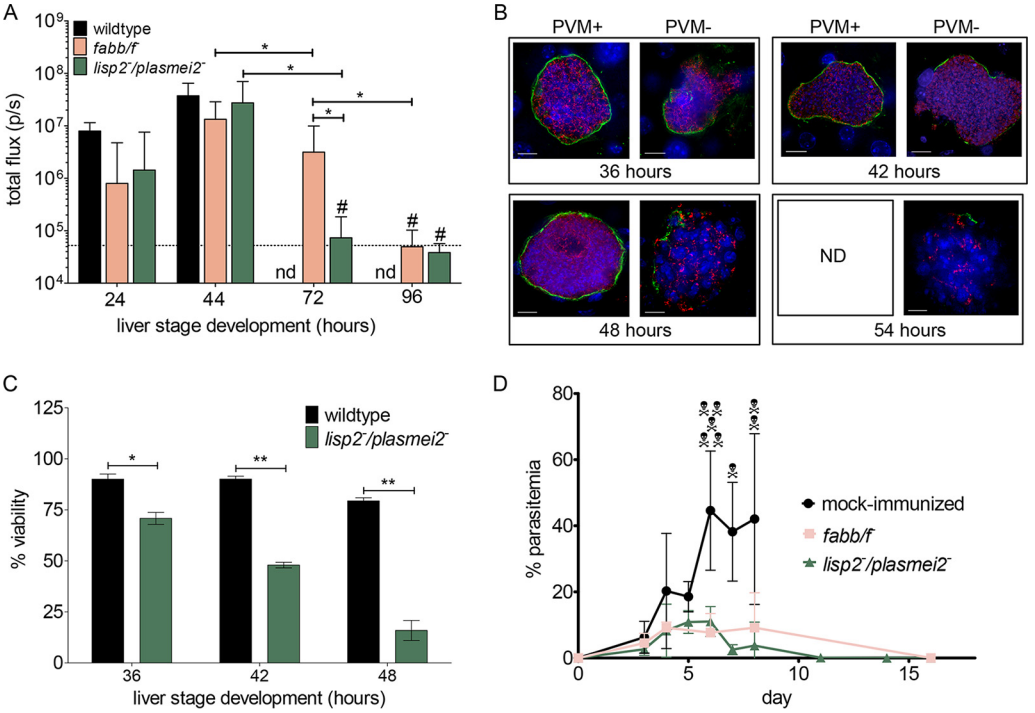

FIG 2 Late-arresting *P. yoelii* GAPs persist and protect from a lethal blood stage challenge. (A) Groups of C57BL/6 mice ($n \geq 6$) were inoculated with 50,000 *P. yoelii* luciferase-expressing wild-type, *fabb/f* $^{-}$, or *lisp2*$^{-}$ *plasmei2*$^{-}$ sporozoites. *In vivo* bioluminescent imaging was used to assay liver stage development (total flux, photons per second [p/s], *y* axis) at 24, 44, 72, and 96 h (*x* axis) after inoculation. Background luminescence is depicted as a dashed horizontal line. Significant differences are shown (*), based on an unpaired two-tailed *t* test where $P < 0.006$. #, flux is not significantly different from background based on an unpaired two-tailed *t* test. nd, not determined due to transition to blood stage. (B) IFA of *lisp2*$^{-}$ *plasmei2*$^{-}$ liver stage schizonts allowed for phenotypic analysis based on the compromised expression of the PVM marker Hep17 (green) (PVM+, complete circumferential expression; PVM−, incomplete). The parasite was further delineated using antibody to the ER marker BiP (red) and staining DNA with DAPI (blue). Scale bar: 10 μm. Analysis took place at 36, 42, 48, and 54 h of development. nd, not detected since all parasites were compromised. (C) The proportion of viable and nonviable wild-type and *lisp2*$^{-}$ *plasmei2*$^{-}$ liver stage schizonts parasites was determined at 36, 42, and 48 h of development. At least 50 parasites in four independent liver sections were counted at each time point. At each time point the *lisp2*$^{-}$ *plasmei2*$^{-}$ liver stages were statistically less viable than the wild type based on an unpaired two-tailed *t* test (*, $P < 0.003$; **, $P < 0.0001$). (D) Groups of C57BL/6 mice were immunized twice with 50,000 intravenous sporozoites (*P. yoelii fabb/f* $^{-}$, 4 mice [pink], and *P. yoelii lisp2*$^{-}$ *plasmei2*$^{-}$, 10 mice [green]) and uninfected salivary gland extract as a control (naive, 8 mice [black]) 1 month apart and i.v. challenged with 10,000 lethal YM *P. yoelii*-infected erythrocytes. Parasitemia was followed until clearance. All naive mice were euthanized to avoid distress when parasitemia exceeded 65% (shown as skull and crossbones).

(Fig. 2C). At 48 h, a time point when wild-type parasites are beginning to transition from liver stage-to-blood stage transition, over 84% of *lisp2*$^{-}$ *plasmei2*$^{-}$ GAP were compromised, compared to only 21% for the wild type (Fig. 2C). By 54 h, all *lisp2*$^{-}$ *plasmei2*$^{-}$ liver stages were compromised based on PVM integrity, and by 60 h, no *lisp2*$^{-}$ *plasmei2*$^{-}$ liver stages were detected, suggesting that *lisp2*$^{-}$ *plasmei2*$^{-}$ liver stages were cleared from the liver by 60 h.

As we had observed the lowest frequency of breakthrough infections among single gene knockouts in the *plasmei2*$^{-}$ parasite, we next determined if comparable high doses of *lisp2*$^{-}$ *plasmei2*$^{-}$ GAP would lead to breakthrough infection. We thus performed challenges i.v. with 200,000 or 500,000 *lisp2*$^{-}$ *plasmei2*$^{-}$ sporozoites in cohorts of highly susceptible BALB/cByJ mice for each dose. We did not observe any breakthrough to blood stage infection (0/29 for 200,000 and 0/26 for 500,000 [Table 1]). This finding shows that the *P. yoelii lisp2*$^{-}$ *plasmei2*$^{-}$ gene knockout combination constitutes a synthetic lethal phenotype in which two sublethal single gene deletions synergize to cause a completely penetrant lethal phenotype. In consequence, the *lisp2*$^{-}$ *plasmei2*$^{-}$ GAP is completely attenuated at late liver stage.

The *P. yoelii lisp2*$^{-}$ *plasmei2*$^{-}$ GAP protects against preerythrocytic and erythrocytic stage challenge. To study preerythrocytic protection, groups of BALB/cJ mice

TABLE 2 *P. yoelii* GAP protect from sporozoite challenge

Strain	GAP genotype	No. of sporozoites used for:			No. of mice protected[c]	No. of sporozoites used for rechallenge[d]	No. of mice protected[c]
		Prime[a]	Boost[a]	Challenge[b]			
BALB/cJ		—[e]	—[e] (60)	10,000 (30)	0/5		
	plasmei2$^-$ *lisp2*$^-$	10,000	10,000 (60)	10,000 (30)	5/5	10,000 (30)	5/5
		—[e]	—[e] (60)	10,000 (40)	0/5		
	plasmei2$^-$ *lisp2*$^-$	10,000	10,000 (90)	10,000 (40)	14/14		
SW		—[e]	—[e] (30, 60)	15 bites (30)	0/5	15 bites (90)[f]	0/5
	plasmei2$^-$ *lisp2*$^-$	50,000	50,000 (30, 60)	15 bites (30)	9/10	15 bites (90)	3/4
	plasmei2$^-$ *lisp2*$^-$	50,000	50,000 (30, 60)	15 bites (180)	4/5		
	fabb/f$^-$	50,000	50,000 (30, 60)	15 bites (30)	10/10	15 bites (90)	3/4

[a]*P. yoelii* GAP salivary gland sporozoites were isolated from infected *Anopheles stephensi* mosquitoes, and mice were i.v. immunized with the listed number of sporozoites. The day(s) after the prime that the boost(s) took place is indicated in parentheses.
[b]Mice were either challenged i.v. with the listed number of wild-type sporozoites or with the listed number of infectious mosquito bites. The days after the last boost the challenge took place are indicated in parentheses.
[c]The number of protected mice per number of mice challenged is indicated. Protection was considered complete if mice remained blood stage negative for 21 days after challenge, based on Giemsa-stained thin blood smear.
[d]Mice were rechallenged i.v. with the listed number of wild-type sporozoites or infectious mosquito bites. The days after the challenge the rechallenge took place are indicated in parentheses.
[e]—, control mice were immunized with comparable amounts of salivary gland extract from uninfected mosquitoes.
[f]Control mice for the rechallenge were a separate cohort.

were i.v. immunized twice at 2- to 3-month intervals with 10,000 *P. yoelii lisp2*$^-$ *plasmei2*$^-$ GAP sporozoites and subsequently i.v. challenged with 10,000 wild-type sporozoites 30 days after the boost (Table 2). Readout of protection was the absence of detectable blood stage parasitemia as determined by thin blood smear microscopy starting 3 days after sporozoite challenge and continuing until day 21. All *P. yoelii lisp2*$^-$ *plasmei2*$^-$ GAP-immunized mice were completely protected from the wild-type sporozoite challenge, and in a subset of mice tested, all mice were protected from a rechallenge 30 days after the first challenge (Table 2). The data demonstrate that the *P. yoelii lisp2*$^-$ *plasmei2*$^-$ GAP affords complete preerythrocytic stage protection and thereby prevents the onset of blood stage parasitemia.

We next conducted immunizations using outbred SW mice, which are inherently more difficult to protect by whole *P. yoelii* sporozoite immunizations than inbred mice (30). We compared the *lisp2*$^-$ *plasmei2*$^-$ GAP with the late liver stage-arresting *fabb/f*$^-$ GAP (27), the current gold standard for preerythrocytic protection in mice. Groups of mice were i.v. immunized three times 1 month apart with 50,000 sporozoites of each GAP and then challenged by the bites of 15 *P. yoelii* wild-type-infected mosquitoes 30 days after the last immunization. Ninety percent of the mice immunized with *P. yoelii lisp2*$^-$ *plasmei2*$^-$ were protected and 100% of the mice immunized with *P. yoelii fabb/f*$^-$ were protected (Table 2), showing that both GAP afford robust protection against the natural route of sporozoite challenge.

To further test durability of protection, we rechallenged a subset of immunized SW mice 5 months after the original mosquito bite challenge. Mice were again challenged by the bite of 15 mosquitoes harboring wild-type *P. yoelii* sporozoites and monitored for development of parasitemia by microscopy for 21 days. None of the naive controls were protected (0/5) and were blood stage positive by day 4 postinfection, while 75% of the *P. yoelii lisp2*$^-$ *plasmei2*$^-$ sporozoite-immunized mice were protected and 75% of the *fabb/f*$^-$ sporozoite-immunized mice were protected (Table 2). In addition, the mice that were not protected became patent at a later time point in comparison with the controls (Table 2). Additionally, long-term durability of protection in a subset of immunized SW mice was assessed with first challenge by mosquito bite 6 months after the last immunization and 80% of mice were protected (Table 2). Taken together, these data demonstrate that immunization of outbred SW mice with late liver stage-arresting GAP induces long-term immune responses that confer robust sterile protection against sporozoite challenge.

Previous work has shown that C57BL/6 mice immunized with *P. yoelii fabb/f*$^-$ were protected from a direct blood stage challenge, whereas early liver stage-arresting

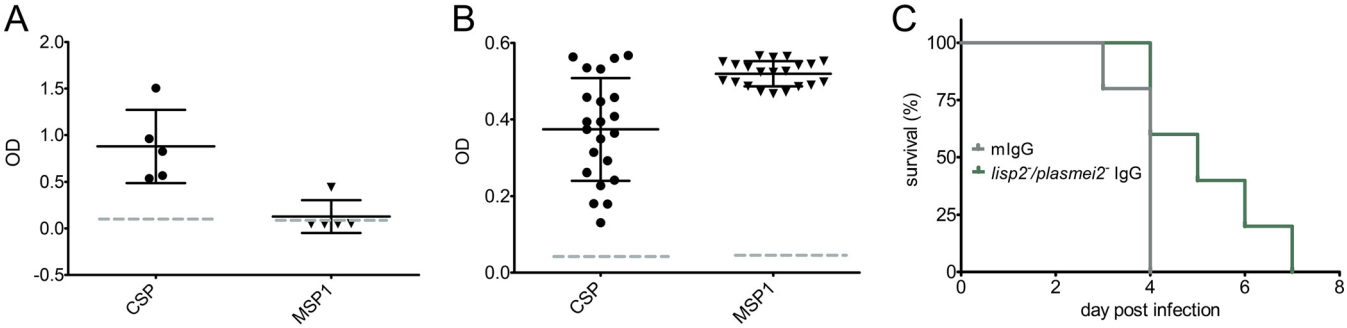

FIG 3 *P. yoelii lisp2*$^{-}$ *plasmei2*$^{-}$ GAP immunization elicits protective humoral responses. (A and B) ELISA was used to measure levels of antibodies that recognize the sporozoite surface marker CSP (left) and the merozoite surface marker MSP1 (right) from the sera of *lisp2*$^{-}$ *plasmei2*$^{-}$ GAP-immunized SW (A) and BALB/cJ (B) mice. The *y* axis shows the OD reading after detection using suitably diluted sera. The dashed line shows the average response from the pooled sera from at least five mock-immunized mice. (C) IgG was isolated from *lisp2*$^{-}$ *plasmei2*$^{-}$ GAP-immunized BALB/cJ mice 45 days after the second immunization and passively transferred i.v. into naive mice. Control mice received the same amount of mouse IgG isolated from naive mice. Twenty-four hours later, the mice were challenged by five infectious mosquito bites and subsequently followed daily (*x* axis) until they became blood stage parasite patent (percent nonpatent, *y* axis). Mice that received IgG from immunized mice became patent later than the control mice ($P < 0.05$ based on the Grehan-Breslow-Wilcoxon test). Each point shows the response from an individual mouse.

parasite immunizations such as with irradiated sporozoites did not protect against a blood stage challenge (31). This suggests that late liver stage-arresting parasites express protective antigens that are shared with blood stages. Since *P. yoelii lisp2*$^{-}$ *plasmei2*$^{-}$ also arrests late in liver stage development, we tested whether groups of C57BL/6 mice that were immunized with 50,000 *P. yoelii lisp2*$^{-}$ *plasmei2*$^{-}$ sporozoites or *P. yoelii fabb/f*$^{-}$ sporozoites 1 month apart were protected from an intravenous challenge of 10,000 lethal *P. yoelii* YM blood stage parasites. Naive mice were unable to control the blood stage infection. Conversely, both the *P. yoelii lisp2*$^{-}$ *plasmei2*$^{-}$ sporozoite-immunized mice and *P. yoelii fabb/f*$^{-}$ sporozoite-immunized mice were protected from the challenge and exhibited a low initial parasitemia before clearing the blood stage parasite infection (Fig. 2D). This result demonstrates that *P. yoelii lisp2*$^{-}$ *plasmei2*$^{-}$ sporozoite immunization engenders stage-transcending protection.

***P. yoelii lisp2*$^{-}$ *plasmei2*$^{-}$ GAP immunization generates parasite-specific antibody and T cell responses. (i) Antibody responses.** Mechanistic studies of preerythrocytic protection after GAP immunization have shown the importance of both antibody-mediated responses that target the sporozoite as well as CD8 T cell-mediated responses that target the liver stage parasites (42, 43). Most rodent malaria studies have been carried out with inbred BALB/c and C57BL/6 mice. Outbred mice are less well studied, but we here show protection against mosquito bite challenge in outbred SW mice after *P. yoelii lisp2*$^{-}$ *plasmei2*$^{-}$ GAP immunization (Table 2). With the knowledge that the natural route of challenge likely allows protective antibodies to block the sporozoite journeys from the bite site to the liver (44), we further investigated the preerythrocytic antibody response in SW mice. Since the circumsporozoite protein (CSP) is an immunodominant sporozoite antigen and antibodies to CSP are protective, we used an enzyme-linked immunosorbent assay (ELISA) readout to determine serum reactivity to full-length *P. yoelii* CSP (44) in groups of five SW mice immunized as before (Table 2). GAP-immunized mice showed high levels of CSP reactivity, whereas mock-immunized mice showed baseline activity (Fig. 3A). This demonstrates that GAP-immunized mice generate robust humoral responses to CSP, indicating the likely importance of antibodies in the preerythrocytic protective immune response after GAP immunization. In addition, since the *P. yoelii lisp2*$^{-}$ *plasmei2*$^{-}$ GAP arrests at a late liver stage developmental time point when exoerythrocytic merozoite formation should be occurring, we determined serum reactivity to the immunodominant blood stage antigen merozoite surface protein 1 (MSP1) (Fig. 3A). Interestingly, there was significant reactivity to this antigen from only one immunized SW mouse, suggesting either that the late-arresting GAP does not express high levels of MSP1 despite the fact that protection from a blood stage challenge was observed or that this antigen does not

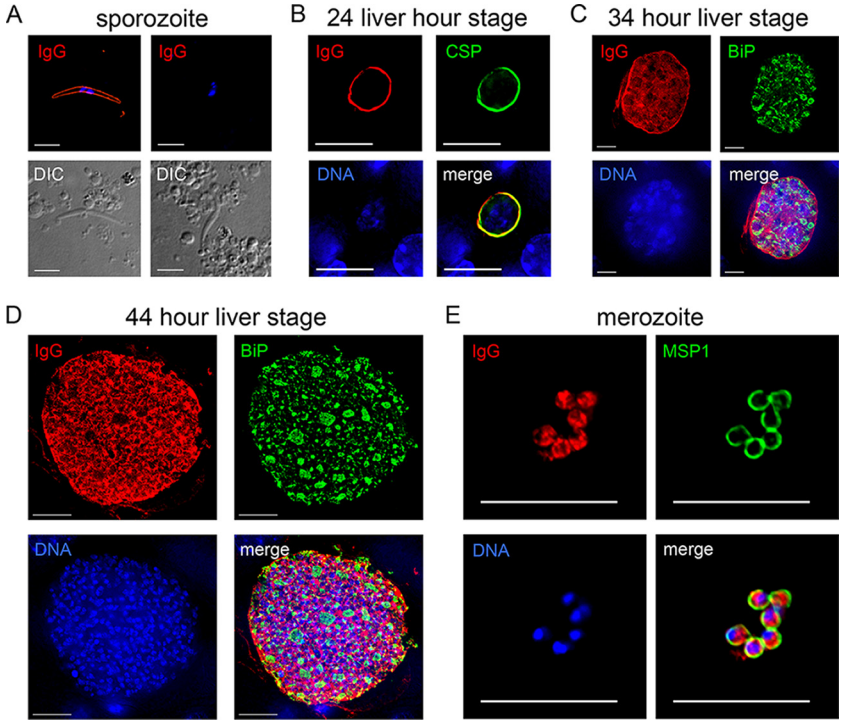

FIG 4 *P. yoelii lisp2*$^{-}$ *plasmei2*$^{-}$ GAP immunization of SW mice elicits humoral responses to multiple life cycle stages. (A to E) IFA was used to determine IgG antibody activity against the parasite from GAP-immunized mice. Sera from five pooled mice were diluted 1:200 for IFA, and bound antibody was detected with a fluorescent secondary antibody. (A) Sera from GAP-immunized mice (IgG, top left, in red) but not sera from naive mice (IgG, top right) recognize the sporozoite surface. Differential interference contrast images of the sporozoites are shown in the bottom images. (B-to D) Liver stage IFAs using GAP-immunized sera (shown in red) show cross-reactivity with CSP (shown in green) at 24 h of development (B) and internal reactivity at 34 (C) and 44 h (D) of development. The parasite was visualized with antibody to BiP (shown in green). (E) GAP-immunized sera recognizes the blood stage merozoite interior, and the merozoite surface was visualized with antibody to MSP1 (green). In panels B to E, DNA is shown in blue. Scale bars in panels A and E represent 5 μm, and those in panels B to D represent 10 μm.

elicit antibodies in the outbred mouse background (Fig. 2D). This suggests that the immune responses that control the blood stage infection in SW mice do not exclusively target MSP1. Alternatively, since the SW mouse is outbred, this could have led to the inconsistent results from the MSP1 ELISA readout using sera from immunized SW mice. We thus repeated the immunization regimen with inbred BALB/cJ mice, which we had already shown to be completely protected (Table 2) from challenge. All immunized mice showed high levels of serum activity to both CSP and MSP1, indicating that a consistent and robust humoral immune response was achieved in inbred BALB/cJ mice (Fig. 3B). Importantly, to determine the level of protection afforded by the humoral immune response, we isolated IgG from the sera of BALB/cJ immunized mice and passively transferred the sera into naive mice as well as transferring similar amounts of nonimmune control IgG into control naive mice (five per group). Twenty-four hours later, the mice were challenged with wild-type infectious *P. yoelii* delivered by mosquito bite, and the time to blood stage patency was determined (Fig. 3C). There was a significant delay to patency in the mice that received IgG from the *lisp2*$^{-}$ *plasmei2*$^{-}$ GAP-immunized mouse cohort, evidence that the IgG could recognize and substantially prevent sporozoite passage from the skin to the liver and thus increase the time to onset of blood stage patency.

To provide further evidence of serum reactivity, we performed IFA initially using pooled sera from the immunized SW mice and showed antibody binding to the sporozoite surface (Fig. 4A), in agreement with the results from the CSP ELISA. To determine if sera could also recognize liver stages and blood stage parasites, IFAs were

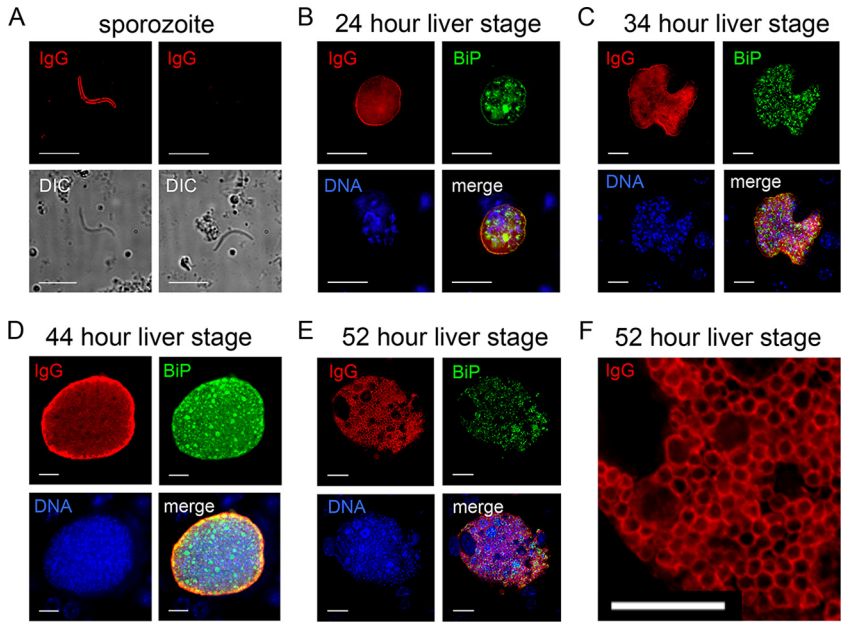

FIG 5 *P. yoelii lisp2*$^{-}$ *plasmei2*$^{-}$ GAP immunization of BALB/cJ mice elicits humoral responses to multiple life cycle stages. (A to F) IFA was used to determine IgG antibody activity against the parasite from GAP-immunized mice. Sera from pooled mice were diluted 1:200 for IFA, and bound antibody was detected with a fluorescent secondary antibody. (A) Sera from GAP-immunized mice (IgG, top left, in red) but not sera from naive mice (IgG, top right) recognize the sporozoite surface. Differential interference contrast images of the sporozoites are shown in the bottom images. (B to D) Liver stage IFAs using GAP-immunized sera (shown in red) show liver stage peripheral and internal reactivities at 24 (B), 34 (C), and 44 (D) h of development. At 52 h (E), sera recognize the surface of exoerythrocytic merozoites in a segmenting schizont, magnified for clarity in panel F. The parasite was visualized with antibody to BiP (shown in green) and DNA in blue. Scale bar: 10 μm.

performed on liver sections from infected mice at 24 h (Fig. 4B), 34 h (Fig. 4C), and 44 h (Fig. 4D) of liver stage development. Early in liver stage development, at 24 h (Fig. 4B), serum reactivity showed a circumferential pattern localization in liver stages similar to CSP. Later on in liver stage development, the sera recognized the parasite periphery (surface and/or parasitophorous vacuole) but also internal structures, suggesting that humoral responses to late liver stage schizonts were also being generated (Fig. 4C and D). In these IFAs, antibody to BiP was used to localize the endoplasmic reticulum of the parasite and minor colocalization with BiP was evident. Importantly, the immune sera also recognized asexual blood stage merozoites (Fig. 4E), and the pattern of recognition was mostly cell internal, based on the sparse colocalization with MSP1, in agreement with the inconsistent lack of serum reactivity to MSP1 (Fig. 3A). Thus, immunization of outbred SW mice with late liver stage-arresting GAP elicited humoral responses that recognize multiple parasite stages.

Since we saw a consistent immune response to MSP1 in immunized BALB/cJ mice (Fig. 3B), we repeated a similar IFA time course on sporozoite and liver stage parasites (Fig. 4) using pooled immune sera to determine the extent of the humoral response (Fig. 5). As with pooled sera from SW immunized mice, there was antibody binding to the sporozoite surface (Fig. 5A), and early in liver stage development, at 24 h (Fig. 5B), serum reactivity showed a circumferential localization although in contrast to the SW-immunized sera, there was also some internal localization. As for SW-immunized sera, later on in liver stage development, the sera recognized the parasite periphery (surface and/or parasitophorous vacuole) but also internal structures, suggesting that humoral responses to late liver stage schizonts were also being generated (Fig. 5C and D). Interestingly and in agreement with the MSP1 ELISA data, the immune sera specifically recognized the exoerythrocytic merozoite surface in segmenting liver stage schizonts (Fig. 5E and F), in contrast to the SW-immunized sera that mostly

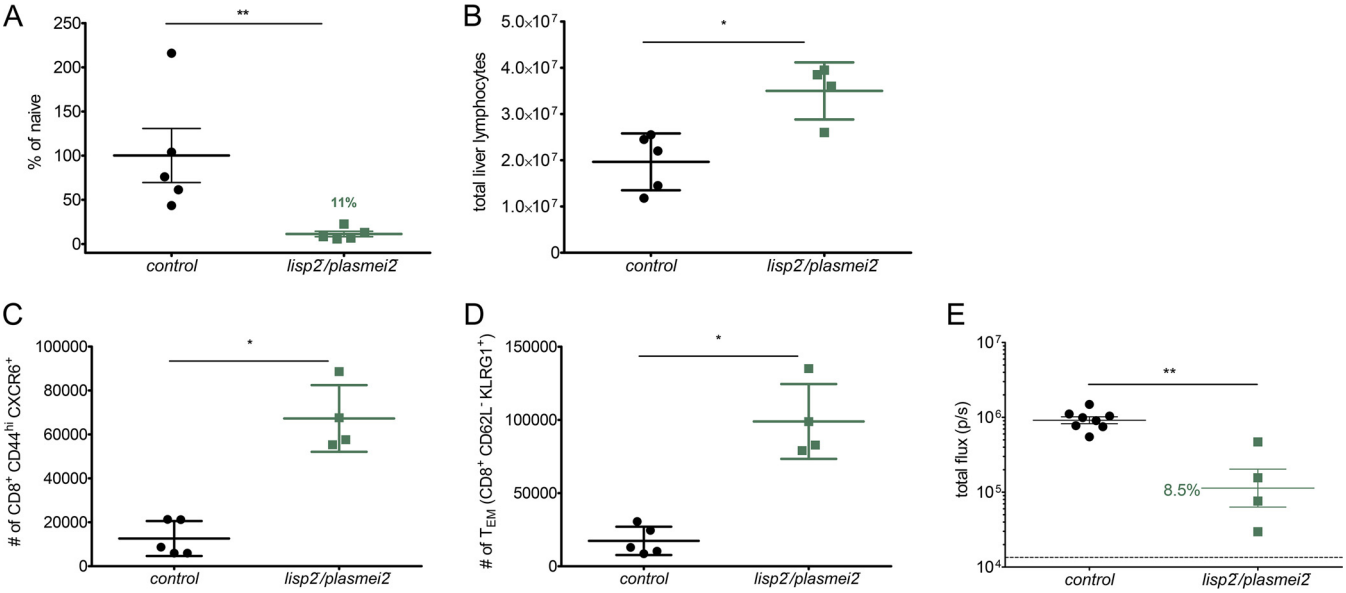

FIG 6 *P. yoelii lisp2*$^{-}$ *plasmei2*$^{-}$ GAP immunization induces long-term liver-specific CD8 T cell immunity. SW mice were immunized three times, challenged after 6 weeks by mosquito bite (Table 2), and then rechallenged i.v. with 7,000 luciferase-expressing *P. yoelii* sporozoites 40 days later. (A) Parasite liver burden was assessed at 42 h postinfection by bioluminescent imaging. (B to D) Mice were sacrificed and their livers perfused for isolation of liver nonparenchymal cells and phenotyping by flow cytometry. The total numbers of liver lymphocytes (B), CD8 T_{EM} ($CD8^+$ $CD62L^-$ $KLRG1^+$ population) (C), and antigen-experienced $CD8^+$ $CXCR6^+$ T cells ($CD8^+$ $CD44^{hi}$ $CXCR6^+$) (D) are shown compared to those in naive, challenged controls. (E) CD8 T cells were isolated from the livers of BALB/cJ 45 days after they had been immunized twice with *lisp2*$^{-}$ *plasmei2*$^{-}$ GAP. A total of 1.5×10^6 liver CD8 T cells from immunized mice and an equivalent number from mock-immunized mice were injected i.v. into naive BALB/cJ mice. Twenty-four hours after the transfer, each mouse was infected i.v. with 1,500 luciferase-expressing wild-type sporozoites. Forty-four hours later, liver stage burden was quantified by *in vivo* bioluminescent imaging (total flux, *y* axis). Each point represents a single mouse. Statistical comparisons were performed by Mann-Whitney U test (*, $P < 0.05$; **, $P < 0.01$).

reacted with internal merozoite antigens (Fig. 4E). Thus, immunization of inbred BALB/cJ mice with *lisp2*$^{-}$ *plasmei2*$^{-}$ late liver stage-arresting GAP elicited humoral responses that recognize the sporozoite, the liver stage parasites, the blood stage parasites, and the exoerythrocytic merozoite surface.

(ii) T cell responses. Numerous studies have shown that immunization with both GAP and RAS elicits protective CD8 T cells (30, 43, 45–50) and CD8 T cell subsets that play critical roles include CD8 effector memory T cells (T_{EM}) (47) as well as CD8 T cells that home to the liver via the chemokine receptor CXCR6 (51, 52). To study CD8 T cell recruitment to the liver after *P. yoelii lisp2*$^{-}$ *plasmei2*$^{-}$ GAP immunization, a subset of SW mice i.v. rechallenged with 7,000 *P. yoelii* GFP-luciferase sporozoites were analyzed for liver stage burden using bioluminescence imaging at 42 h after the challenge. Immunized mice had a significantly reduced liver stage burden, 89% $\pm$ 6.9%, compared to that of control naive mice (Fig. 6A), demonstrating the efficacy of the immune response in eliminating liver stage parasites. The mice were then sacrificed immediately following the measurement of parasite liver burden, and their livers were perfused for phenotyping of liver-resident CD8 T cells by flow cytometry. Immunized mouse livers contained significantly more total lymphocytes than challenged naive controls (Fig. 6B). Importantly, the livers of immunized mice had increases in CD8 T_{EM} (5.7-fold increase) (Fig. 6C), known to be important in mounting rapid responses to infected hepatocytes. In addition, we also observed increased numbers of antigen-experienced $CD44^{hi}$ $CXCR6^+$ CD8 T cells (5.2-fold increase) (Fig. 6D) in the liver, suggesting the significance of these liver-resident CD8 T cells in mounting an effective cellular response against infected hepatocytes. To further assay the importance of CD8 T cells for protection, CD8 T cells from the livers of *lisp2*$^{-}$ *plasmei2*$^{-}$ GAP-immunized BALB/cJ mice were adoptively transferred to naive mice and these mice were subsequently challenged with *P. yoelii* wild-type infectious sporozoites by mosquito bite. Control naive mice received CD8 T cells from mock-immunized mice. To assay the ability of the transferred T cells to prevent liver stage development, luciferase activity was measured at 44 h. The liver

stage burden in mice with adoptively transferred T cells from immunized mice had a significantly reduced mean liver stage burden, 91.5%, compared to control mice (Fig. 6E), demonstrating the role of liver-resident CD8 T cells from immunized mice in eliminating liver stage parasites. Taken together, these data demonstrate that *lisp2*$^{-}$ *plasmei2*$^{-}$ GAP immunization of mice induces protracted, liver-resident memory CD8 T cell responses that are important in providing robust protection.

DISCUSSION

Attenuated preerythrocytic *P. falciparum* malaria parasites engender immune responses that protect human subjects from an infectious sporozoite challenge (10, 19, 53, 54). Their clinical testing was inspired and built on extensive research studies with attenuated preerythrocytic stages of the rodent malaria parasites *P. yoelii* and *P. berghei* (11, 27, 55, 56). Attenuation was first achieved by the irradiation of sporozoites, but more recently, genetic attenuation by precise gene deletion(s) has been possible. Whereas sporozoite irradiation, by means of random DNA damage, causes the uncontrolled early arrest of the liver stage parasite before extensive DNA replication, genetic attenuation has design potential and, depending on the gene deletion, could arrest the liver stage parasite at any point during its development. While first-generation GAP were built by gene deletion(s) of loci that control the early stages of hepatocyte infection, thereby causing early liver stage arrest, the deletion of genes encoding fatty acid biosynthesis (FAS II) in rodent malaria parasites caused arrest late in liver stage development (27, 28). The distinct liver stage growth arrest phenotypes allowed for comparisons of the immunogenicity and efficacy of late liver stage-arresting attenuated rodent malaria GAP to early liver stage-arresting rodent malaria RAS and GAP. These studies showed that not only could late liver stage-arresting GAP confer superior protection against homologous sporozoite challenge in inbred and outbred mice, but also they protected mice against a heterologous rodent malaria sporozoite challenge and a lethal blood stage challenge (30, 31, 44). The enhanced protection is likely mediated by a diversification of the antigenic targets of the protective CD8 T cell response and the antibody responses, demonstrating the importance of both arms of the immune system in this unprecedented protection. These findings provide a convincing rationale for the development of a late liver stage-arresting *P. falciparum* GAP as an optimal live-attenuated vaccine. Unfortunately, however, FAS II gene deletions in *P. falciparum* prevent sporozoite formation (32, 33), and in consequence such a vaccine cannot be produced.

We continued our search for gene deletions that cause a late liver stage-arresting phenotype and attempted to combine gene deletions that in concert would yield a completely attenuated GAP. Here we have shown that a novel *P. yoelii* GAP, created by deletion of *lisp2* and *plasmei2*, is a synthetic lethal and completely arrests the parasite late in liver stage development. Although deletion of either gene alone is not sufficient to arrest liver stage development completely, resulting in infrequent breakthrough blood stage infection, the simultaneous deletion of both genes causes complete growth arrest and death of the parasite. Typically in synthetic lethality, a single gene deletion does not have a profound effect on phenotype, but this is not always the case. In our studies, the *PlasMei2* deletion had a pronounced phenotype and only showed liver stage-to-blood stage breakthrough in a small subset of susceptible BALB/cByJ mice, whereas the *LISP2* deletion was less deleterious and even a relatively small dose of 1,000 sporozoites administered i.v. led to patency in less susceptible BALB/cJ mice. It appears counterintuitive that combining a gene deletion associated with a strong attenuation phenotype with a gene deletion with a weak attenuation phenotype would result in complete attenuation. Nevertheless, this synergistic effect was observed in the dual loss of gene function, but how precisely the *LISP2* and *PlasMei2* gene deletions interact—the former functioning at the liver stage parasitophorous vacuole (37) and the latter in RNA homeostasis (34)—to severely impact parasite development remains to be determined. The postgenomic tools of systems biology allow for the functional characterization of genes through understanding gene-gene interactions, as well as

interactions between biological pathways, and exploiting synthetic lethality can aid in the investigation of these interactions. Synthetic lethal screening is a powerful technique and has been used with great success in model organisms such as *Saccharomyces cerevisiae* (57), *Drosophila melanogaster* (58), and *Caenorhabditis elegans* (59) and is currently being pursued for cancer therapy (60). The rationale behind such screens is that the deletion of two genes whose interaction is essential will result in lethality, whereas the gene deletions on their own can be tolerated. Gene-gene interactions in *Plasmodium* are poorly understood, particularly for the liver stage parasite. Research in this arena could aid in the discovery of further gene-gene interactions that could be perturbed for the purpose of GAP creation. Rapid, successive gene deletions in *Plasmodium* are now possible with CRISPR/Cas9 technology (40, 61, 62), and thus, the creation of multilocus-attenuated late liver stage-arresting GAP is within reach.

We found that immunization with *P. yoelii lisp2*$^-$ *plasmei2*$^-$ completely protects against sporozoite challenge and also confers stage-transcending protection against a lethal blood stage challenge. The breadth and duration of the immune responses engendered by *P. yoelii lisp2*$^-$ *plasmei2*$^-$ vaccination might be vital for the breadth of protection. *lisp2*$^-$ *plasmei2*$^-$ GAP immunization elicited antibodies that recognized the sporozoite surface, including CSP, known to be critical for humoral protection against sporozoite infection, and provided projection from mosquito bite challenge after passive transfer. Immune sera also recognized the liver stages at 24, 34, and 44 h of development as well as blood stage parasites. Although it is not clear if antibody recognition of the liver stage parasite plays a role in protection, antibody recognition of the blood stage parasite is an important component of the stage-transcending protection provided by late liver stage-arresting GAP, as previously shown for the *P. yoelii fabb/f*$^-$ GAP (31). Indeed, *P. yoelii lisp2*$^-$ *plasmei2*$^-$ was as protective as *P. yoelii fabb/f*$^-$ against a lethal blood stage challenge. This suggests that the induction of stage-transcending protection is a universal feature of late liver stage-arresting GAP and appears not to depend on the particular gene knockout that causes the attenuation.

Sterile immunity engendered by attenuated parasite vaccination is critically dependent on CD8 T cells that target the liver stage-infected hepatocytes. Recently, it has been shown that in addition to CD8 T_{EM} cells, liver-resident CD8 T cells also play a vital role in protection (47, 52, 63, 64). We observed that *P. yoelii lisp2*$^-$ *plasmei2*$^-$ GAP immunization led to significant increases in antigen-experienced CD8 T_{EM} cells and liver-resident CD8 T cells. These CD8 T cells undoubtedly play a significant role in conferring robust sterile protection. We showed this by adoptive transfer of CD8 T cells from *lisp2*$^-$ *plasmei2*$^-$ GAP-immunized mice into naive mice, which dramatically reduced liver stage burden after i.v. sporozoite challenge. This mode of challenge largely bypasses the humoral protection that plays a role in preventing sporozoites from exiting the skin after mosquito bite infection.

The enhanced magnitude and breadth of protective immune responses that is observed with late liver stage-arresting GAP provides advantages compared to early liver stage-arresting parasites. Of clinical significance, the immunizing dose of sporozoites required to achieve protection is lower. Thus, the number of sporozoites per immunization can be decreased and/or the total number of immunizations can be decreased without leading to a loss of sterile protection against infection. In addition, immune responses confer protection against heterologous challenge and may even show cross-species protection, as has been demonstrated for immunization with the late liver stage-arresting *P. yoelii fabb/f*$^-$ GAP, which protected against a *P. berghei* challenge (30). Finally, the demonstration that *P. yoelii lisp2*$^-$ *plasmei2*$^-$ immunization protects from a lethal, heterologous blood stage challenge raises the hope that even if sterile protection against preerythrocytic infection wanes, stage-transcending protection could prevent fulminant blood stage replication and consequently alleviate malaria disease. Ultimately, a late liver stage-arresting *P. falciparum lisp2*$^-$ *plasmei2*$^-$ strain has yet to be generated, and with both the *lisp2* gene and *plasmei2* gene showing high

conservation among malaria parasites it is possible to pursue such a promising GAP in *P. falciparum* for human vaccination.

MATERIALS AND METHODS

Experimental animals. Six- to 8-week-old female SW mice from Harlan (Indianapolis, IN) were used for parasite life cycle maintenance and production of transgenic parasites. Six- to 8-week-old female BALB/cAnN mice from Harlan were used for assessments indirect immunofluorescence assays (IFAs). Six- to 8-week-old female BALB/cJ and BALB/cByJ mice from the Jackson Laboratory (Bar Harbor, ME) were used to assess the attenuation and ability of parasites to act as experimental vaccines. *P. yoelii* parent and transgenic parasites were cycled between SW mice and *Anopheles stephensi* mosquitoes for the purposes of sporozoite production. Infected mosquitoes were maintained on sugar water at 24°C and 70% humidity. This study was carried out in strict accordance with the recommendations in the *Guide for the Care and Use of Laboratory Animals* of the National Research Council (65). The Center for Infectious Disease Research has an OLAW Animal Welfare Assurance (A3640-01). The protocol was approved by the Center for Infectious Disease Research Institutional Animal Care and Use Committee.

Creation of *P. yoelii lisp2*$^-$, *lisp2*$^-$ *plasmei2*$^-$, and *fabb/f*$^-$. All oligonucleotide primers used for the creation and analyses of parasites are detailed in Table S1 in the supplemental material. Deletion of *P. yoelii LISP2* was achieved based on the previously reported CRISPR/Cas9 strategy using plasmid pYC (40). In brief, *LISP2* was deleted using double-crossover homologous recombination following a double-stranded DNA break mediated by Cas9 containing a guide RNA targeting the gene of interest. Complementary regions upstream and downstream of the open reading frame were ligated into plasmid pYC, as was the 20-nucleotide guide RNA sequence (40), resulting in the creation of plasmid pYC_LISP2. The pYC plasmid was transfected into the blood stage schizonts of *P. yoelii* line 1971cl1 (41), a marker-free parasite that behaves as the wild type and expresses a green fluorescent protein (GFP)-luciferase fusion throughout the life cycle under the control of the elongation factor 1 alpha promoter. This led to the creation of the *P. yoelii lisp2*$^-$. Two separate knockout clones from two independent transfections were initially phenotypically analyzed throughout the life cycle. To create *P. yoelii lisp2*$^-$ *plasmei2*$^-$, the plasmid originally used to create *P. yoelii plasmei2*$^-$, pL0034_PlasMei2 (34), was transfected into the marker-free *P. yoelii lisp2*$^-$ parasite and two clones from separate transfections were isolated for further analysis. To achieve deletion of *FabB/F*, the GIMO technology used to create *P. yoelii plasmei2*$^-$ was used and the pL0034_FabB/F plasmid was transfected into the blood stage schizonts of the luciferase-expressing *P. yoelii* line 1971cl1 (41).

After transfection of all parasites and intravenous injection into SW mice, pyrimethamine was used for the positive selection and downstream cloning of recombinant parasites using standard techniques (66). Transgenesis was confirmed by PCR using methodology we have used on multiple occasions (see reference 25 for a recent example).

Immunofluorescence analysis. (i) Liver stage. BALB/cAnN mice were injected i.v. with approximately 3×10^5 sporozoites, and livers were harvested from euthanized mice at several time points postinfection. Livers were perfused with 1× phosphate-buffered saline (PBS) and fixed in 4% (vol/vol) paraformaldehyde (PFA) in 1× PBS, and lobes were cut into 50-μm sections using a Vibratome apparatus (Ted Pella, Redding, CA). For IFA, sections were permeabilized in 1× Tris-buffered saline (TBS) containing 3% (vol/vol) H_2O_2 and 0.25% (vol/vol) Triton X-100 for 30 min at room temperature. Sections were then blocked in 1× TBS containing 5% (wt/vol) dried milk (TBS-M) for at least 1 h and incubated with primary antibody in TBS-M at 4°C overnight. After a washing in 1× TBS, fluorescent secondary antibodies were added in TBS-M for 2 h at room temperature in a manner similar to that described above. After a further washing, the section was incubated in 0.06% (wt/vol) $KMnO_4$ for 2 min to quench background fluorescence. Sections were then washed with 1× TBS and stained with 1 μg/ml of 4,6-diamidino-2-phenylindole (DAPI) in 1× TBS for 5 to 10 min at room temperature to visualize DNA and mounted with FluoroGuard anti-fade reagent (Bio-Rad, Hercules, CA).

(ii) Sporozoite. Salivary gland sporozoites were extracted from infected mosquitoes, washed once in 1× PBS, fixed in 4% (vol/vol) paraformaldehyde (PFA) in 1× PBS, and allowed to dry onto 12-well microscope slides. Sporozoites were permeabilized and blocked with 3% bovine serum albumin (BSA) and 0.25% Triton X-100 in 1× PBS, washed three times in 1× PBS, and incubated with a 1:200 dilution of mixed sera from five mock-immunized and five GAP-immunized mice. After an hour, sporozoites were washed three times with 1× PBS, and fluorescent secondary antibodies were added in 1× PBS for 1 h at room temperature in a manner similar to that described above. Sporozoites were stained with 4 μg/ml of DAPI in 1× PBS to visualize DNA, washed once with 1× PBS, and mounted with FluoroGuard antifade reagent (Bio-Rad, Hercules, CA).

(iii) Blood stage. Infected erythrocytes were processed for IFA using a previously described method (67). Erythrocytes were pelleted initially (and between all steps) at 2,000 × *g* in a microcentrifuge at room temperature for 1 min. Cells were washed twice in 1× PBS, fixed in 1× PBS plus 4% (vol/vol) PFA plus 0.0075% (vol/vol) glutaraldehyde for 30 min at room temperature, and permeabilized in 1× PBS plus 0.2% (vol/vol) Triton X-100 for 10 min at room temperature. A 1× PBS plus 3% (wt/vol) BSA (blocking solution) was applied at 4°C overnight. Primary antibodies were diluted in blocking solution and incubated for 1 h with end-over-end rotation at room temperature. Following two washes with 1× PBS, fluorescent secondary antibodies were diluted in blocking solution and incubated with cells for 30 min with end-over-end rotation at room temperature and shielding from light. Nucleic acid was then stained with DAPI in 1× PBS for 5 to 10 min at room temperature. Cells were washed three times with 1× PBS and mounted with FluoroGuard antifade reagent (Bio-Rad, Hercules, CA).

All preparations were analyzed for fluorescence using a fluorescence inverted microscope (Eclipse TE2000-E; Nikon), and images were acquired using Olympus 1 × 70 DeltaVision deconvolution microscopy.

Phenotypic analysis of *P. yoelii* liver stages. After IFA, liver stage size was measured by determining the area of the parasite at its greatest circumference. Viability was measured by examining the integrity of the parasitophorous vacuole membrane (PVM) marker Hep17. If Hep17 expression did not completely delineate the PVM, the parasite was considered nonviable. Liver stage development was also measured using an *in vivo* imaging system (IVIS) since the parasites used in this study express luciferase and are thus bioluminescent. Luciferase activity in animals was visualized through imaging of whole bodies using the IVIS Lumina II animal imager (Caliper Life Sciences, USA) as previously described (68–70). Mice were injected with 100 μl of RediJect D-luciferin (PerkinElmer) intraperitoneally prior to being anesthetized using the isoflurane anesthesia system (XGI-8; Caliper Life Sciences). Measurements were performed within 5 to 10 min after the injection of D-luciferin. Bioluminescence imaging was acquired with a 10-cm field of view (FOV), medium binning factor, and an exposure time of 1 to 5 min. Quantitative analysis of bioluminescence was performed by measuring the luminescence signal intensity using the region of interest (ROI) settings of the Living Image 3.0 software. ROIs were placed around the whole animal and ROI measurements were expressed as total flux (photons/second).

Sporozoite inoculation and challenge. Sporozoites were isolated from the salivary glands of infected *A. stephensi* mosquitoes between 14 and 18 days after the infectious blood meal and injected i.v. into the tail veins of recipient mice. For assessment of attenuation, sporozoites were injected into highly susceptible BALB/cByJ mice (39). Liver stage-to-blood stage transition (blood stage patency) was assessed by Giemsa-stained thin blood smear starting at day 3 after inoculation and ending at day 21, at which time negative smear was attributed to complete attenuation. For immunizations, C57BL/6, BALB/cJ, and SW mice were primed and boosted with *P. yoelii* sporozoites and subsequently challenged i.v. with *P. yoelii* XNL sporozoites or by *P. yoelii* XNL infectious mosquito bite. Breakthrough to blood stage patency was assessed by Giemsa-stained thin blood smear starting at day 3 after challenge and ending at day 21, at which time a negative smear was attributed to complete protection. Mice immunized only with mosquito salivary gland extract were used as controls.

Blood stage challenge. Frozen stocks of *P. yoelii* YM-infected blood were injected intraperitoneally into C57BL/6 mice and allowed to develop for 2 to 4 days until parasitemia reached a maximum of 1% as determined by Giemsa-stained thin smear. These mice were terminally bled via cardiac puncture and the blood was diluted in PBS to contain 10,000 infected erythrocytes/200 μl. Infected erythrocytes were then injected i.v. at a volume of 200 μl/mouse into immunized recipient mice. Parasitemia was monitored by Giemsa-stained thin smears beginning on day 3 postinfection. Mice were euthanized when parasitemia reached 60% or became moribund.

ELISA. Anti-*P. yoelii* CSP and MSP1 ELISA was conducted as previously described (31). Briefly, high-binding 96-well plates were coated with 1 μg/ml of full-length *P. yoelii* CSP or MSP1. After blocking for 1 h at room temperature, serum samples from immunized and naive mice were added at desired dilutions for 2 h at room temperature. After washing, horseradish peroxidase (HRP)-conjugated anti-mouse IgG secondary antibody was then added at a 1:5,000 dilution for 1 h at room temperature. Plates were developed for using SigmaFast OPD (*o*-phenylenediamine dihydrochloride) for 12 min and optical density (OD) was read at a wavelength of 450 nm.

Analysis of liver lymphocytes. For analysis of liver lymphocytes, liver nonparenchymal cells were isolated as previously described (71). Briefly, mice were anesthetized with ketamine-xylazine prior to perfusion of the liver with 7.5 ml of Hanks' balanced salt solution (HBSS) with 5 mM HEPES and 0.5 mM EDTA followed by 7.5 ml of 0.5-mg/ml collagenase in HBSS with 5 mM HEPES. Nonparenchymal cells were then isolated from liver homogenates by gradient separation using 40% iodixanol. Total lymphocytes per liver were then counted, and up to 8×10^6 liver lymphocytes in 50 μl of PBS–1% fetal bovine serum (FBS) were stained with the following anti-mouse antibodies on ice for 1 h: CD8 Alexa Fluor 488, CD44 peridinin chlorophyll protein (PerCP)-Cy5.5, CD127 brilliant violet 421, CD62L brilliant violet 605, B220 brilliant violet 785, CD3 allophycocyanin (APC), CD4 APC-Cy7, CXCR6 phycoerythrin (PE), and KLRG1 PE-Cy7. Cells were then washed and run on a BD LSRII using FlowJo analysis software. Calculations of total number of cells were determined by expressing the cell type of interest as a percentage of lymphocytes based on forward and side scatter (FSC/SSC) and multiplying this number by the number of lymphocytes counted from each liver.

Adoptive transfer of liver-resident CD8 T cells. Liver lymphocytes were isolated as described above (under " Analysis of liver lymphocytes"), and CD8 T cells were enriched by negative selection using the Easy Sep mouse CD8 T cell enrichment kit (StemCell Technologies, Vancouver, BC, Canada). For the adoptive transfer of CD8 T cells, 1.5×10^6 liver CD8 T cells from immunized mice and an equivalent number from mock-immunized mice were injected i.v. into naive BALB/cJ mice. Twenty-four hours after the transfer, each mouse was infected i.v. with 1,500 luciferase-expressing wild-type sporozoites. Forty-four hours later, mature parasite liver stage burden was quantified by *in vivo* bioluminescent imaging as described above (under "Phenotypic analysis of *P. yoelii* liver stages").

Passive transfer of IgG. Sera were isolated from *lisp2*$^-$ *plasmei2*$^-$ GAP-immunized BALB/cJ mice 45 days after the second immunization. Serum was used for the extraction of IgG using GraviTrap protein G columns (GE Healthcare Life Sciences) following the manufacturer's protocol and concentrated using Amicon Ultra-15 centrifugal units (EMD Millipore) to 20 to 25 mg/ml in PBS. Two milligrams of IgG was passively transferred to mice i.v. Twenty-four hours later, mice were challenged by infectious mosquito bite challenge. Purified nonspecific murine IgG (Sigma) in PBS was used as a negative control.

SUPPLEMENTAL MATERIAL

Supplemental material for this article may be found at https://doi.org/10.1128/IAI.00088-18.

SUPPLEMENTAL FILE 1, PDF file, 0.1 MB.

ACKNOWLEDGMENTS

We thank Heather Kain for help with mosquito rearing as well as the vivarium staff at the Center for Infectious Disease Research for help with rodents. We are indebted to Jing Yuan, Xiamen University, China, for the pYC plasmid used for the knockout of *LISP2*.

This work was supported by NIH grant R01 AI125706 to S.H.I.K.

REFERENCES

1. Olotu A, Fegan G, Wambua J, Nyangweso G, Leach A, Lievens M, Kaslow DC, Njuguna P, Marsh K, Bejon P. 2016. Seven-year efficacy of RTS,S/AS01 malaria vaccine among young African children. N Engl J Med 374:2519–2529. https://doi.org/10.1056/NEJMoa1515257.
2. Clemens J, Moorthy V. 2016. Implementation of RTS,S/AS01 malaria vaccine—the need for further evidence. N Engl J Med 374:2596–2597. https://doi.org/10.1056/NEJMe1606007.
3. White MT, Verity R, Griffin JT, Asante KP, Owusu-Agyei S, Greenwood B, Drakeley C, Gesase S, Lusingu J, Ansong D, Adjei S, Agbenyega T, Ogutu B, Otieno L, Otieno W, Agnandji ST, Lell B, Kremsner P, Hoffman I, Martinson F, Kamthunzu P, Tinto H, Valea I, Sorgho H, Oneko M, Otieno K, Hamel MJ, Salim N, Mtoro A, Abdulla S, Aide P, Sacarlal J, Aponte JJ, Njuguna P, Marsh K, Bejon P, Riley EM, Ghani AC. 2015. Immunogenicity of the RTS,S/AS01 malaria vaccine and implications for duration of vaccine efficacy: secondary analysis of data from a phase 3 randomised controlled trial. Lancet Infect Dis 15:1450–1458. https://doi.org/10.1016/S1473-3099(15)00239-X.
4. RTS/S Clinical Trials Partnership. 2015. Efficacy and safety of RTS,S/AS01 malaria vaccine with or without a booster dose in infants and children in Africa: final results of a phase 3, individually randomised, controlled trial. Lancet 386:31–45. https://doi.org/10.1016/S0140-6736(15)60721-8.
5. Rosenthal PJ. 2015. The RTS,S/AS01 vaccine continues to show modest protection against malaria in African infants and children. Evid Based Med 20(5):179. https://doi.org/10.1136/ebmed-2015-110231.
6. RTS/S Clinical Trials Partnership. 2014. Efficacy and safety of the RTS,S/AS01 malaria vaccine during 18 months after vaccination: a phase 3 randomized, controlled trial in children and young infants at 11 African sites. PLoS Med 11:e1001685. https://doi.org/10.1371/journal.pmed.1001685.
7. Hodgson SH, Ewer KJ, Bliss CM, Edwards NJ, Rampling T, Anagnostou NA, de Barra E, Havelock T, Bowyer G, Poulton ID, de Cassan S, Longley R, Illingworth JJ, Douglas AD, Mange PB, Collins KA, Roberts R, Gerry S, Berrie E, Moyle S, Colloca S, Cortese R, Sinden RE, Gilbert SC, Bejon P, Lawrie AM, Nicosia A, Faust SN, Hill AV. 2015. Evaluation of the efficacy of ChAd63-MVA vectored vaccines expressing circumsporozoite protein and ME-TRAP against controlled human malaria infection in malaria-naive individuals. J Infect Dis 211:1076–1086. https://doi.org/10.1093/infdis/jiu579.
8. Clyde DF, Most H, McCarthy VC, Vanderberg JP. 1973. Immunization of man against sporozite-induced falciparum malaria. Am J Med Sci 266:169–177. https://doi.org/10.1097/00000441-197309000-00002.
9. Seder RA, Chang LJ, Enama ME, Zephir KL, Sarwar UN, Gordon IJ, Holman LA, James ER, Billingsley PF, Gunasekera A, Richman A, Chakravarty S, Manoj A, Velmurugan S, Li M, Ruben AJ, Li T, Eappen AG, Stafford RE, Plummer SH, Hendel CS, Novik L, Costner PJ, Mendoza FH, Saunders JG, Nason MC, Richardson JH, Murphy J, Davidson SA, Richie TL, Sedegah M, Sutamihardja A, Fahle GA, Lyke KE, Laurens MB, Roederer M, Tewari K, Epstein JE, Sim BK, Ledgerwood JE, Graham BS, Hoffman SL, VRC 312 Study Team. 2013. Protection against malaria by intravenous immunization with a nonreplicating sporozoite vaccine. Science 341:1359–1365. https://doi.org/10.1126/science.1241800.
10. Clyde DF. 1990. Immunity to falciparum and vivax malaria induced by irradiated sporozoites: a review of the University of Maryland studies, 1971–75. Bull World Health Organ 68(Suppl):9–12.
11. Mueller AK, Labaied M, Kappe SH, Matuschewski K. 2005. Genetically modified Plasmodium parasites as a protective experimental malaria vaccine. Nature 433:164–167. https://doi.org/10.1038/nature03188.
12. Roestenberg M, McCall M, Hopman J, Wiersma J, Luty AJ, van Gemert GJ, van de Vegte-Bolmer M, van Schaijk B, Teelen K, Arens T, Spaarman L, de Mast Q, Roeffen W, Snounou G, Renia L, van der Ven A, Hermsen CC, Sauerwein R. 2009. Protection against a malaria challenge by sporozoite inoculation. N Engl J Med 361:468–477. https://doi.org/10.1056/NEJMoa0805832.
13. Mordmüller B, Surat G, Lagler H, Chakravarty S, Ishizuka AS, Lalremruata A, Gmeiner M, Campo JJ, Esen M, Ruben AJ, Held J, Calle CL, Mengue JB, Gebru T, Ibanez J, Sulyok M, James ER, Billingsley PF, Natasha KC, Manoj A, Murshedkar T, Gunasekera A, Eappen AG, Li T, Stafford RE, Li M, Felgner PL, Seder RA, Richie TL, Sim BK, Hoffman SL, Kremsner PG. 2017. Sterile protection against human malaria by chemoattenuated PfSPZ vaccine. Nature 542:445–449. https://doi.org/10.1038/nature21060.
14. Bijker EM, Bastiaens GJ, Teirlinck AC, van Gemert GJ, Graumans W, van de Vegte-Bolmer M, Siebelink-Stoter R, Arens T, Teelen K, Nahrendorf W, Remarque EJ, Roeffen W, Jansens A, Zimmerman D, Vos M, van Schaijk BC, Wiersma J, van der Ven AJ, de Mast Q, van Lieshout L, Verweij JJ, Hermsen CC, Scholzen A, Sauerwein RW. 2013. Protection against malaria after immunization by chloroquine prophylaxis and sporozoites is mediated by preerythrocytic immunity. Proc Natl Acad Sci U S A 110:7862–7867. https://doi.org/10.1073/pnas.1220360110.
15. Khan SM, Janse CJ, Kappe SH, Mikolajczak SA. 2012. Genetic engineering of attenuated malaria parasites for vaccination. Curr Opin Biotechnol 23:908–916. https://doi.org/10.1016/j.copbio.2012.04.003.
16. Matuschewski K, Ross J, Brown SM, Kaiser K, Nussenzweig V, Kappe SH. 2002. Infectivity-associated changes in the transcriptional repertoire of the malaria parasite sporozoite stage. J Biol Chem 277:41948–41953. https://doi.org/10.1074/jbc.M207315200.
17. Mueller AK, Camargo N, Kaiser K, Andorfer C, Frevert U, Matuschewski K, Kappe SH. 2005. Plasmodium liver stage developmental arrest by depletion of a protein at the parasite-host interface. Proc Natl Acad Sci U S A 102:3022–3027. https://doi.org/10.1073/pnas.0408442102.
18. Mikolajczak SA, Lakshmanan V, Fishbaugher M, Camargo N, Harupa A, Kaushansky A, Douglass AN, Baldwin M, Healer J, O'Neill M, Phuong T, Cowman A, Kappe SH. 2014. A next-generation genetically attenuated Plasmodium falciparum parasite created by triple gene deletion. Mol Ther 22:1707–1715. https://doi.org/10.1038/mt.2014.85.
19. Kublin JG, Mikolajczak SA, Sack BK, Fishbaugher ME, Seilie A, Shelton L, VonGoedert T, Firat M, Magee S, Fritzen E, Betz W, Kain HS, Dankwa DA, Steel RW, Vaughan AM, Noah Sather D, Murphy SC, Kappe SH. 2017. Complete attenuation of genetically engineered Plasmodium falciparum sporozoites in human subjects. Sci Transl Med 9(371):eaad9099. https://doi.org/10.1126/scitranslmed.aad9099.
20. van Schaijk BC, Ploemen IH, Annoura T, Vos MW, Foquet L, van Gemert GJ, Chevalley-Maurel S, van de Vegte-Bolmer M, Sajid M, Franetich JF, Lorthiois A, Leroux-Roels G, Meuleman P, Hermsen CC, Mazier D, Hoffman SL, Janse CJ, Khan SM, Sauerwein RW. 2014. A genetically attenuated malaria vaccine candidate based on P. falciparum b9/slarp gene-deficient sporozoites. Elife 3:e03582.
21. Rijpma SR, van der Velden M, Gonzalez-Pons M, Annoura T, van Schaijk BC, van Gemert GJ, van den Heuvel JJ, Ramesar J, Chevalley-Maurel S, Ploemen IH, Khan SM, Franetich JF, Mazier D, de Wilt JH, Serrano AE, Russel FG, Janse CJ, Sauerwein RW, Koenderink JB, Franke-Fayard BM. 2016. Multidrug ATP-binding cassette transporters are essential for he-

patic development of Plasmodium sporozoites. Cell Microbiol 18:369–383. https://doi.org/10.1111/cmi.12517.
22. Tarun AS, Peng X, Dumpit RF, Ogata Y, Silva-Rivera H, Camargo N, Daly TM, Bergman LW, Kappe SH. 2008. A combined transcriptome and proteome survey of malaria parasite liver stages. Proc Natl Acad Sci U S A 105:305–310. https://doi.org/10.1073/pnas.0710780104.
23. Waller RF, Keeling PJ, Donald RG, Striepen B, Handman E, Lang-Unnasch N, Cowman AF, Besra GS, Roos DS, McFadden GI. 1998. Nuclear-encoded proteins target to the plastid in Toxoplasma gondii and Plasmodium falciparum. Proc Natl Acad Sci U S A 95:12352–12357.
24. Falkard B, Kumar TR, Hecht LS, Matthews KA, Henrich PP, Gulati S, Lewis RE, Manary MJ, Winzeler EA, Sinnis P, Prigge ST, Heussler V, Deschermeier C, Fidock D. 2013. A key role for lipoic acid synthesis during Plasmodium liver stage development. Cell Microbiol 15:1585–1604. https://doi.org/10.1111/cmi.12137.
25. Lindner SE, Sartain MJ, Hayes K, Harupa A, Moritz RL, Kappe SH, Vaughan AM. 2014. Enzymes involved in plastid-targeted phosphatidic acid synthesis are essential for Plasmodium yoelii liver-stage development. Mol Microbiol 91:679–693. https://doi.org/10.1111/mmi.12485.
26. Pei Y, Tarun AS, Vaughan AM, Herman RW, Soliman JM, Erickson-Wayman A, Kappe SH. 2010. Plasmodium pyruvate dehydrogenase activity is only essential for the parasite's progression from liver infection to blood infection. Mol Microbiol 75:957–971. https://doi.org/10.1111/j.1365-2958.2009.07034.x.
27. Vaughan AM, O'Neill MT, Tarun AS, Camargo N, Phuong TM, Aly AS, Cowman AF, Kappe SH. 2009. Type II fatty acid synthesis is essential only for malaria parasite late liver stage development. Cell Microbiol 11:506–520. https://doi.org/10.1111/j.1462-5822.2008.01270.x.
28. Yu M, Kumar TR, Nkrumah LJ, Coppi A, Retzlaff S, Li CD, Kelly BJ, Moura PA, Lakshmanan V, Freundlich JS, Valderramos JC, Vilcheze C, Siedner M, Tsai JH, Falkard B, Sidhu AB, Purcell LA, Gratraud P, Kremer L, Waters AP, Schiehser G, Jacobus DP, Janse CJ, Ager A, Jacobs WR, Jr, Sacchettini JC, Heussler V, Sinnis P, Fidock DA. 2008. The fatty acid biosynthesis enzyme FabI plays a key role in the development of liver-stage malarial parasites. Cell Host Microbe 4:567–578. https://doi.org/10.1016/j.chom.2008.11.001.
29. Aly AS, Mikolajczak SA, Rivera HS, Camargo N, Jacobs-Lorena V, Labaied M, Coppens I, Kappe SH. 2008. Targeted deletion of SAP1 abolishes the expression of infectivity factors necessary for successful malaria parasite liver infection. Mol Microbiol 69:152–163. https://doi.org/10.1111/j.1365-2958.2008.06271.x.
30. Butler NS, Schmidt NW, Vaughan AM, Aly AS, Kappe SH, Harty JT. 2011. Superior antimalarial immunity after vaccination with late liver stage-arresting genetically attenuated parasites. Cell Host Microbe 9:451–462. https://doi.org/10.1016/j.chom.2011.05.008.
31. Sack BK, Keitany GJ, Vaughan AM, Miller JL, Wang R, Kappe SH. 2015. Mechanisms of stage-transcending protection following immunization of mice with late liver stage-arresting genetically attenuated malaria parasites. PLoS Pathog 11:e1004855. https://doi.org/10.1371/journal.ppat.1004855.
32. Cobbold SA, Vaughan AM, Lewis IA, Painter HJ, Camargo N, Perlman DH, Fishbaugher M, Healer J, Cowman AF, Kappe SH, Llinas M. 2013. Kinetic flux profiling elucidates two independent acetyl-CoA biosynthetic pathways in Plasmodium falciparum. J Biol Chem 288:36338–36350. https://doi.org/10.1074/jbc.M113.503557.
33. van Schaijk BC, Kumar TR, Vos MW, Richman A, van Gemert GJ, Li T, Eappen AG, Williamson KC, Morahan BJ, Fishbaugher M, Kennedy M, Camargo N, Khan SM, Janse CJ, Sim KL, Hoffman SL, Kappe SH, Sauerwein RW, Fidock DA, Vaughan AM. 2014. Type II fatty acid biosynthesis is essential for Plasmodium falciparum sporozoite development in the midgut of Anopheles mosquitoes. Eukaryot Cell 13:550–559. https://doi.org/10.1128/EC.00264-13.
34. Dankwa DA, Davis MJ, Kappe SH, Vaughan AM. 2016. A Plasmodium yoelii Mei2-like RNA binding protein is essential for completion of liver stage schizogony. Infect Immun 84:1336–1345. https://doi.org/10.1128/IAI.01417-15.
35. Annoura T, van Schaijk BC, Ploemen IH, Sajid M, Lin JW, Vos MW, Dinmohamed AG, Inaoka DK, Rijpma SR, van Gemert GJ, Chevalley-Maurel S, Kielbasa SM, Scheltinga F, Franke-Fayard B, Klop O, Hermsen CC, Kita K, Gego A, Franetich JF, Mazier D, Hoffman SL, Janse CJ, Sauerwein RW, Khan SM. 2014. Two Plasmodium 6-Cys family-related proteins have distinct and critical roles in liver-stage development. FASEB J 28:2158–2170. https://doi.org/10.1096/fj.13-241570.
36. Kumar H, Sattler JM, Singer M, Heiss K, Reinig M, Hammerschmidt-Kamper C, Heussler V, Mueller AK, Frischknecht F. 2016. Protective efficacy and safety of liver stage attenuated malaria parasites. Sci Rep 6:26824. https://doi.org/10.1038/srep26824.
37. Orito Y, Ishino T, Iwanaga S, Kaneko I, Kato T, Menard R, Chinzei Y, Yuda M. 2013. Liver-specific protein 2: a Plasmodium protein exported to the hepatocyte cytoplasm and required for merozoite formation. Mol Microbiol 87:66–79. https://doi.org/10.1111/mmi.12083.
38. Egel R, Nielsen O, Weilguny D. 1990. Sexual differentiation in fission yeast. Trends Genet 6:369–373. https://doi.org/10.1016/0168-9525(90)90279-F.
39. Kaushansky A, Austin LS, Mikolajczak SA, Lo FY, Miller JL, Douglass AN, Arang N, Vaughan AM, Gardner MJ, Kappe SH. 2015. Susceptibility to Plasmodium yoelii preerythrocytic infection in BALB/c substrains is determined at the point of hepatocyte invasion. Infect Immun 83:39–47. https://doi.org/10.1128/IAI.02230-14.
40. Zhang C, Xiao B, Jiang Y, Zhao Y, Li Z, Gao H, Ling Y, Wei J, Li S, Lu M, Su XZ, Cui H, Yuan J. 2014. Efficient editing of malaria parasite genome using the CRISPR/Cas9 system. mBio 5:e01414-14. https://doi.org/10.1128/mBio.01414-14.
41. Lin JW, Annoura T, Sajid M, Chevalley-Maurel S, Ramesar J, Klop O, Franke-Fayard BM, Janse CJ, Khan SM. 2011. A novel 'gene insertion/marker out' (GIMO) method for transgene expression and gene complementation in rodent malaria parasites. PLoS One 6:e29289. https://doi.org/10.1371/journal.pone.0029289.
42. Dups JN, Pepper M, Cockburn IA. 2014. Antibody and B cell responses to Plasmodium sporozoites. Front Microbiol 5:625. https://doi.org/10.3389/fmicb.2014.00625.
43. Schmidt NW, Podyminogin RL, Butler NS, Badovinac VP, Tucker BJ, Bahjat KS, Lauer P, Reyes-Sandoval A, Hutchings CL, Moore AC, Gilbert SC, Hill AV, Bartholomay LC, Harty JT. 2008. Memory CD8 T cell responses exceeding a large but definable threshold provide long-term immunity to malaria. Proc Natl Acad Sci U S A 105:14017–14022. https://doi.org/10.1073/pnas.0805452105.
44. Keitany GJ, Sack B, Smithers H, Chen L, Jang IK, Sebastian L, Gupta M, Sather DN, Vignali M, Vaughan AM, Kappe SH, Wang R. 2014. Immunization of mice with live-attenuated late liver stage-arresting Plasmodium yoelii parasites generates protective antibody responses to preerythrocytic stages of malaria. Infect Immun 82:5143–5153. https://doi.org/10.1128/IAI.02320-14.
45. Montagna GN, Beigier-Bompadre M, Becker M, Kroczek RA, Kaufmann SH, Matuschewski K. 2014. Antigen export during liver infection of the malaria parasite augments protective immunity. mBio 5:e01321-14. https://doi.org/10.1128/mBio.01321-14.
46. Tse SW, Radtke AJ, Zavala F. 2011. Induction and maintenance of protective CD8+ T cells against malaria liver stages: implications for vaccine development. Mem Inst Oswaldo Cruz 106(Suppl 1):S172–S178. https://doi.org/10.1590/S0074-02762011000900022.
47. Reyes-Sandoval A, Wyllie DH, Bauza K, Milicic A, Forbes EK, Rollier CS, Hill AV. 2011. CD8+ T effector memory cells protect against liver-stage malaria. J Immunol 187:1347–1357. https://doi.org/10.4049/jimmunol.1100302.
48. Schmidt NW, Butler NS, Badovinac VP, Harty JT. 2010. Extreme CD8 T cell requirements for anti-malarial liver-stage immunity following immunization with radiation attenuated sporozoites. PLoS Pathog 6:e1000998. https://doi.org/10.1371/journal.ppat.1000998.
49. Cockburn IA, Chen YC, Overstreet MG, Lees JR, van Rooijen N, Farber DL, Zavala F. 2010. Prolonged antigen presentation is required for optimal CD8+ T cell responses against malaria liver stage parasites. PLoS Pathog 6:e1000877. https://doi.org/10.1371/journal.ppat.1000877.
50. Overstreet MG, Cockburn IA, Chen YC, Zavala F. 2008. Protective CD8 T cells against Plasmodium liver stages: immunobiology of an 'unnatural' immune response. Immunol Rev 225:272–283. https://doi.org/10.1111/j.1600-065X.2008.00671.x.
51. Pichyangkul S, Spring MD, Yongvanitchit K, Kum-Arb U, Limsalakpetch A, Im-Erbsin R, Ubalee R, Vanachayangkul P, Remarque EJ, Angov E, Smith PL, Saunders DL. 2017. Chemoprophylaxis with sporozoite immunization in P. knowlesi rhesus monkeys confers protection and elicits sporozoite-specific memory T cells in the liver. PLoS One 12:e0171826. https://doi.org/10.1371/journal.pone.0171826.
52. Tse SW, Radtke AJ, Espinosa DA, Cockburn IA, Zavala F. 2014. The chemokine receptor CXCR6 is required for the maintenance of liver memory CD8(+) T cells specific for infectious pathogens. J Infect Dis 210:1508–1516. https://doi.org/10.1093/infdis/jiu281.
53. Behet MC, Foquet L, van Gemert GJ, Bijker EM, Meuleman P, Leroux-Roels G, Hermsen CC, Scholzen A, Sauerwein RW. 2014. Sporozoite

immunization of human volunteers under chemoprophylaxis induces functional antibodies against pre-erythrocytic stages of Plasmodium falciparum. Malar J 13:136. https://doi.org/10.1186/1475-2875-13-136.
54. Lyke KE, Ishizuka AS, Berry AA, Chakravarty S, DeZure A, Enama ME, James ER, Billingsley PF, Gunasekera A, Manoj A, Li M, Ruben AJ, Li T, Eappen AG, Stafford RE, Kc N, Murshedkar T, Mendoza FH, Gordon IJ, Zephir KL, Holman LA, Plummer SH, Hendel CS, Novik L, Costner PJ, Saunders JG, Berkowitz NM, Flynn BJ, Nason MC, Garver LS, Laurens MB, Plowe CV, Richie TL, Graham BS, Roederer M, Sim BK, Ledgerwood JE, Hoffman SL, Seder RA. 2017. Attenuated PfSPZ vaccine induces strain-transcending T cells and durable protection against heterologous controlled human malaria infection. Proc Natl Acad Sci U S A 114:2711–2716. https://doi.org/10.1073/pnas.1615324114.
55. Labaied M, Harupa A, Dumpit RF, Coppens I, Mikolajczak SA, Kappe SH. 2007. Plasmodium yoelii sporozoites with simultaneous deletion of P52 and P36 are completely attenuated and confer sterile immunity against infection. Infect Immun 75:3758–3768. https://doi.org/10.1128/IAI.00225-07.
56. van Dijk MR, Douradinha B, Franke-Fayard B, Heussler V, van Dooren MW, van Schaijk B, van Gemert GJ, Sauerwein RW, Mota MM, Waters AP, Janse CJ. 2005. Genetically attenuated, P36p-deficient malarial sporozoites induce protective immunity and apoptosis of infected liver cells. Proc Natl Acad Sci U S A 102:12194–12199. https://doi.org/10.1073/pnas.0500925102.
57. Baetz K, Measday V, Andrews B. 2006. Revealing hidden relationships among yeast genes involved in chromosome segregation using systematic synthetic lethal and synthetic dosage lethal screens. Cell Cycle 5:592–595. https://doi.org/10.4161/cc.5.6.2583.
58. Wheeler DB, Bailey SN, Guertin DA, Carpenter AE, Higgins CO, Sabatini DM. 2004. RNAi living-cell microarrays for loss-of-function screens in Drosophila melanogaster cells. Nat Methods 1:127–132. https://doi.org/10.1038/nmeth711.
59. Lamitina T. 2006. Functional genomic approaches in C. elegans. Methods Mol Biol 351:127–138.
60. Thompson JM, Nguyen QH, Singh M, Razorenova OV. 2015. Approaches to identifying synthetic lethal interactions in cancer. Yale J Biol Med 88:145–155.
61. Wagner JC, Platt RJ, Goldfless SJ, Zhang F, Niles JC. 2014. Efficient CRISPR-Cas9-mediated genome editing in Plasmodium falciparum. Nat Methods 11:915–918. https://doi.org/10.1038/nmeth.3063.
62. Ghorbal M, Gorman M, Macpherson CR, Martins RM, Scherf A, Lopez-Rubio JJ. 2014. Genome editing in the human malaria parasite Plasmodium falciparum using the CRISPR-Cas9 system. Nat Biotechnol 32:819–821. https://doi.org/10.1038/nbt.2925.
63. Cabrera M, Pewe LL, Harty JT, Frevert U. 2013. In vivo CD8+ T cell dynamics in the liver of Plasmodium yoelii immunized and infected mice. PLoS One 8:e70842. https://doi.org/10.1371/journal.pone.0070842.
64. Fernandez-Ruiz D, Ng WY, Holz LE, Ma JZ, Zaid A, Wong YC, Lau LS, Mollard V, Cozijnsen A, Collins N, Li J, Davey GM, Kato Y, Devi S, Skandari R, Pauley M, Manton JH, Godfrey DI, Braun A, Tay SS, Tan PS, Bowen DG, Koch-Nolte F, Rissiek B, Carbone FR, Crabb BS, Lahoud M, Cockburn IA, Mueller SN, Bertolino P, McFadden GI, Caminschi I, Heath WR. 2016. Liver-resident memory CD8+ T cells form a front-line defense against malaria liver-stage infection. Immunity 45:889–902. https://doi.org/10.1016/j.immuni.2016.08.011.
65. National Research Council. 2011. Guide for the care and use of laboratory animals, 8th ed. National Academies Press, Washington, DC.
66. Janse CJ, Ramesar J, Waters AP. 2006. High-efficiency transfection and drug selection of genetically transformed blood stages of the rodent malaria parasite Plasmodium berghei. Nat Protoc 1:346–356. https://doi.org/10.1038/nprot.2006.53.
67. Tonkin CJ, van Dooren GG, Spurck TP, Struck NS, Good RT, Handman E, Cowman AF, McFadden GI. 2004. Localization of organellar proteins in Plasmodium falciparum using a novel set of transfection vectors and a new immunofluorescence fixation method. Mol Biochem Parasitol 137:13–21. https://doi.org/10.1016/j.molbiopara.2004.05.009.
68. Franke-Fayard B, Waters AP, Janse CJ. 2006. Real-time in vivo imaging of transgenic bioluminescent blood stages of rodent malaria parasites in mice. Nat Protoc 1:476–485. https://doi.org/10.1038/nprot.2006.69.
69. Mwakingwe A, Ting LM, Hochman S, Chen J, Sinnis P, Kim K. 2009. Noninvasive real-time monitoring of liver-stage development of bioluminescent Plasmodium parasites. J Infect Dis 200:1470–1478. https://doi.org/10.1086/606115.
70. Ploemen IH, Prudencio M, Douradinha BG, Ramesar J, Fonager J, van Gemert GJ, Luty AJ, Hermsen CC, Sauerwein RW, Baptista FG, Mota MM, Waters AP, Que I, Lowik CW, Khan SM, Janse CJ, Franke-Fayard BM. 2009. Visualisation and quantitative analysis of the rodent malaria liver stage by real-time imaging. PLoS One 4:e7881. https://doi.org/10.1371/journal.pone.0007881.
71. Miller JL, Sack BK, Baldwin M, Vaughan AM, Kappe SH. 2014. Interferon-mediated innate immune responses against malaria parasite liver stages. Cell Rep 7:436–447. https://doi.org/10.1016/j.celrep.2014.03.018.